

Interaction induced dimerization in zigzag single wall carbon nanotubes

Sam T. Carr,¹ Alexander O. Gogolin,² and Alexander A. Nersesyan^{3,4}

¹*School of Physics and Astronomy, University of Birmingham, Birmingham B15 2TT, United Kingdom*

²*Department of Mathematics, Imperial College, 180 Queen's Gate, London SW7 2BZ, United Kingdom*

³*The Abdus Salam International Centre for Theoretical Physics, 34100, Trieste, Italy*

⁴*The Andronikashvili Institute of Physics, Tamarashvili 6, 0177, Tbilisi, Georgia*

(Dated: October 30, 2018)

We derive a low-energy effective model of metallic zigzag carbon nanotubes at half filling. We show that there are three important features characterizing the low-energy properties of these systems: the long-range Coulomb interaction, umklapp scattering and an explicit dimerization generated by interactions. The ratio of the dimerization induced gap and the Mott gap induced by the umklapp interactions is dependent on the radius of the nanotube and can drive the system through a quantum phase transition with $SU(2)_1$ quantum symmetry. We consider the physical properties of the phases on either side of this transition which should be relevant for realistic nanotubes.

PACS numbers: 71.10.Pm, 73.63.Fg

I. INTRODUCTION

Since their discovery,¹ carbon nanotubes have attracted a great amount of attention, both theoretically and experimentally.² It is widely appreciated that single-wall nanotubes (SWNT) constitute almost ideal systems where peculiar effects specific to strong correlations in one dimension (1D) can be observed. They are structurally 1D objects built by wrapping a sheet of graphene into a cylinder. The type of wrapping is characterized by the superlattice vector (n, m) . From the point of view of strong correlations metallic nanotubes are of particular interest. In the absence of interactions between the electrons,³ the band structure is indeed metallic for all (n, n) (or *armchair*) nanotubes, as well as for the $(n, -n)$ (or *zigzag*) nanotubes with n being multiple of 3. In all other cases there is band gap which at large n is of the order of $(10/n)eV$.

The low-energy effective theory for correlated metallic SWNTs away from half-filling⁴ shows that the long-range Coulomb interaction converts the nanotubes into Tomonaga-Luttinger liquids implying various scaling laws for conductance, which have since been verified experimentally.⁵ At half-filling the effects of strong correlations become even more pronounced in the presence of the poorly screened Coulomb interaction. The latter makes the umklapp scattering processes strongly relevant giving rise to sizable Mott gaps.⁶ The underlying strong-coupling phases for armchair nanotubes were recently classified in Ref. 7.

In this paper, we study the effects of the long-range Coulomb interaction in half-filled zigzag SWNTs (n divisible by 3). The new feature that makes this case qualitatively different from the armchair nanotubes is an explicit dimerization that originates from the nearest-neighbor interaction and gives rise to a single-particle gap of the order of $1/n$. Notice that curvature effects,⁸ which are known to lead to much smaller band gaps, $\sim 1/n^2$, can therefore be safely neglected. We will explain how the dimerization comes about, discuss its interplay with the

Mott gaps and show that this competition can result in a quantum phase transition similar to the one studied previously in the context of dimerized spin ladders.^{9,10} Making reasonable approximations for the relative strengths of different interaction terms for a zigzag SWNT shows that the system can occur very close to the quantum criticality, and may even be tuned to reach it by changing the radius of the nanotube; however a realistic estimation of the parameters by either experiment or numerical techniques is beyond the scope of this paper.

Below we will follow the same strategy as in the armchair case⁷ paying particular attention to the differences. The structure of the paper is as follows: First we consider the band-structure of the zigzag SWNT within a tight-binding model and show that, in the low-energy limit, the latter is equivalent to an effective two-chain model. We then very carefully consider the structure of the interaction, taking into account both the long-range tail of the unscreened Coulomb interaction and the details of the short-range component of the interaction which depend in an important way on the lattice. We then solve this model by using bosonization, employing the adiabatic approximation to treat neutral collective excitations, and then concentrating on energies well below the charge gap, by refermionizing the remaining theory. This allows us to identify the nature of the phase transition generated by the dimerization term, and extract some physical properties of such nanotubes.

II. MAPPING ONTO LOW ENERGY EFFECTIVE THEORY

In this section, we single out those two bands that cross the Fermi level in an undoped isolated zigzag SWNT, which allows us to describe the relevant part of the spectrum in terms of an equivalent two-chain fermionic model. We carefully analyze the details of the lattice structure that determine the peculiarities of the interaction terms. We then pass to the continuum limit and em-

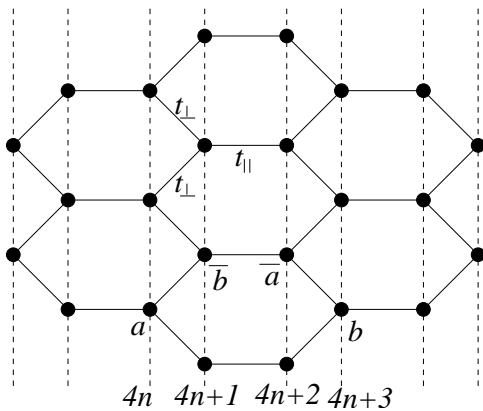


FIG. 1: Real space structure of a zigzag nanotube. In this paper the chain direction is chosen to be x , meaning that the axis of the graphite sheet have been rotated by 90° as compared to the references that deal with the armchair case.

ploy the bosonization technique to derive the low-energy effective field theory for a metallic zigzag SWNT.

A. Kinetic term and two chain model in zigzag nanotubes

We begin with a tight-binding model on the honeycomb graphite lattice shown in Fig.1. The structure consists of an underlying triangular lattice with two inequivalent Carbon positions, labeled by a and b . It proves convenient to double the unit cell such that the new cell contains four atoms, a, \bar{b}, \bar{a}, b . In this picture the unit cell is rectangular, so the two momenta, k_x and k_y , can be considered as independent. Wrapping a $(N \times n)$ graphite sheet into a $(n, -n)$ zigzag nanotube quantizes the electron momentum in the direction of the superlattice vector $\mathbf{C} = n(\mathbf{a}_1 - \mathbf{a}_2)$, i.e. the y direction in our Cartesian axis. Carrying out a partial Fourier transform in this direction gives a Hamiltonian describing n 1D bands (see e.g. Ref. 11),

$$H_0 = - \sum_q \sum_{l=1}^{4N} t_q(l) [c_q^\dagger(l) c_q(l+1) + h.c.]. \quad (1)$$

Here l labels the sites of an effective 1D lattice along the tube's axis, the lattice spacing being $x_{l+1} - x_l \equiv b = \sqrt{3}/4$, q is the band index taking n integer values ($|q| < n/2$), and $t_q(l) = t_0(q) + (-1)^l \Delta(q)$ is an alternating hopping amplitude whose uniform and staggered parts are given by

$$t_0(q) = \frac{1}{2} [t_{\parallel} + 2t_{\perp} \cos(\pi q/n)], \quad (2)$$

$$\Delta(q) = \frac{1}{2} [t_{\parallel} - 2t_{\perp} \cos(\pi q/n)]. \quad (3)$$

Thus the spectrum is generically gapped, the gap of the q th band being determined by the dimerization am-

plitude (3). However, for two bands labeled by $q = \pm Q = \pm n/3$ ($n = 3m$) the gap is minimal, proportional to the difference $t_{\parallel} - t_{\perp}$, and is solely due to curvature effects. This difference was shown⁸ to be of the order $1/n^2$ and is much smaller than the gaps of all the other bands. For this reason, and also in view of the fact that the interactions are of the order $1/n$ or larger, one can set $t_{\parallel} = t_{\perp}$ and thus make the lowest-energy part of the spectrum described in terms of two decoupled, translationally invariant chains with a simple half-filled cosine band, via the mapping

$$\begin{aligned} b(m_x, m_y) &\rightarrow \frac{1}{\sqrt{n}} [e^{iQy} c_+(4m_x) + e^{-iQy} c_-(4m_x)] \\ a(m_x, m_y) &\rightarrow \frac{1}{\sqrt{n}} [e^{iQy} c_+(4m_x + 1) + e^{-iQy} c_-(4m_x + 1)] \\ \bar{b}(m_x, m_y) &\rightarrow \frac{1}{\sqrt{n}} [e^{iQ(y+1/2)} c_+(4m_x + 2) \\ &\quad + e^{-iQ(y+1/2)} c_-(4m_x + 2)] \\ \bar{a}(m_x, m_y) &\rightarrow \frac{1}{\sqrt{n}} [e^{iQ(y+1/2)} c_+(4m_x + 3) \\ &\quad + e^{-iQ(y+1/2)} c_-(4m_x + 3)]. \end{aligned} \quad (4)$$

This picture is in contrast with the case of armchair nanotubes where the kinetic part of the low-energy theory is that of two strongly coupled chains (ladder). Even though curvature effects can be neglected, the dimerization Δ should be retained in the Hamiltonian. This follows from the fact that interactions generate an identical term in the low-energy effective theory, but with a much larger amplitude, $\sim 1/n$. The next two sections will demonstrate this phenomena, which is one of the central results of this paper.

B. Interactions

There are two important contributions to the interactions. Firstly, in an isolated nanotube, the Coulomb interaction is unscreened, so one must take into account the effects of its long-range tail. Secondly, at half-filling, Umklapp processes originating from the short-range part of the Coulomb interaction play a crucial role. Below we consider these two contributions separately.

The long-range part of the interaction is insensitive to the details of the lattice and is simply given by

$$H_{\text{Coul}} = \sum_{l'l'} n(l) U(l-l') n(l'), \quad (5)$$

where $n(l) = \sum_{\mu\sigma} c_{\mu\sigma}^\dagger c_{\mu\sigma}$ is the total density on lattice site l in the two chain mapping, and $U(x) \sim e^2/|x|$.

The effects of the short-range part of the interaction are best elucidated by considering the minimal model that captures all essential physics of the problem. It turns out that a two-parameter model with on-site (U) and

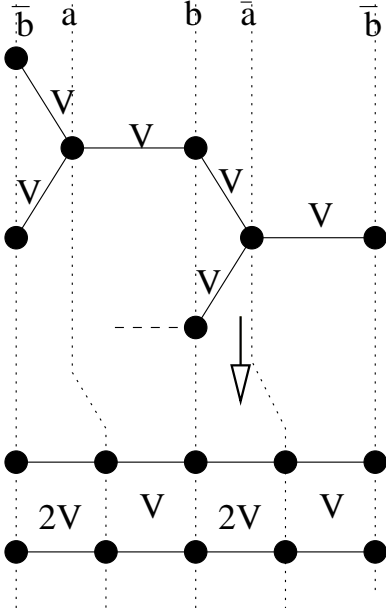


FIG. 2: A cartoon representation of the origin of the staggered interaction

nearest-neighbour (V) couplings fully represents the most general structure of local interaction in the low-energy limit,

$$H_1 = U \sum_{m_x, m_y} n_{\uparrow}(m_x, m_y) n_{\downarrow}(m_x, m_y) + V \sum_{\langle n, n' \rangle} n(m_x, m_y) n(m'_x, m'_y). \quad (6)$$

Here m_x, m_y label the carbon atoms on the original 2D lattice, the summation in the second term goes over nearest neighbours, and $n(m_x, m_y) = n_{\uparrow}(m_x, m_y) + n_{\downarrow}(m_x, m_y)$ is the electron density on site (m_x, m_y) . When the V -term is projected onto the two low-energy chains, we see an interesting effect as illustrated in Fig. 2: each atom a (\bar{a}) interacts with one atom b (\bar{b}) and with two atoms \bar{b} (b). In other words, when mapping onto the two-chain low-energy sector, the interaction $V_{ab} = V_{\bar{a}\bar{b}} \neq V_{a\bar{b}} = V_{\bar{a}b}$. This means that in the low-energy theory the V interaction will contain not only a uniform part but also a staggered part. The latter is entirely due to the way we break the C_3 symmetry of the 2D lattice by wrapping it to form a zigzag nanotube; the effect is not present in the armchair case. Carrying out the mapping (4) to the effective two-chain model, with index $\mu = \pm$ labeling the two chains, yields three terms,

$$H_U = \frac{U}{n} \sum_{l\mu} n_{\mu\uparrow}(l) n_{\mu\downarrow}(l) + \frac{U}{n} \sum_{l\mu} c_{\mu\uparrow}^\dagger c_{-\mu\uparrow} c_{-\mu\downarrow}^\dagger c_{\mu\downarrow}$$

$$H_V = \frac{3V}{2n} \sum_l n(l) n(l+1)$$

$$H_s = -\frac{V}{2n} \sum_l (-1)^l n(l) n(l+1) + \frac{V}{n} \sum_{l\mu\sigma\sigma'} (-1)^l c_{\mu\sigma}^\dagger c_{-\mu\sigma} c_{-\mu\sigma'}^\dagger c_{\mu\sigma'}, \quad (7)$$

where H_U is the contribution from the on-site interaction, H_V is the smooth contribution from the nearest neighbor interaction, and H_s is the staggered part of the nearest neighbor interaction. We now proceed to study the ground state and elementary excitations of such an interacting two chain model by employing the bosonization technique.

C. Chiral Decomposition and Bosonization

Passing to the continuum limit, we adopt the standard description in terms of chiral (right/left) fermions. At half-filling $k_F = \pm\pi/2b$, so that

$$c_{\mu\sigma}(l) \rightarrow \sqrt{b} [i^l R_{\mu\sigma}(x) + (-i)^l L_{\mu\sigma}(x)], \quad (8)$$

where $\sigma = \uparrow, \downarrow$ is the spin index. This yields $H_0 = \int dx \mathcal{H}_0(x)$, where

$$\mathcal{H}_0 = -iv_F (R_{\mu\sigma}^\dagger \partial_x R_{\mu\sigma} - L_{\mu\sigma}^\dagger \partial_x L_{\mu\sigma}) + 2g_\Delta \mathcal{O}_{\text{dim}},$$

$$\mathcal{O}_{\text{dim}} = i (R_{\mu\sigma}^\dagger L_{\mu\sigma} - L_{\mu\sigma}^\dagger R_{\mu\sigma}). \quad (9)$$

To treat interactions nonperturbatively, we employ Abelian bosonization based on the correspondence $R(L)_{\mu\sigma} \rightarrow (2\pi\alpha)^{-1/2} \exp[-i\sqrt{\pi}(\Phi_{\mu\sigma} \mp \Theta_{\mu\sigma})]$, where $\Phi_{\mu\sigma}$ and $\Theta_{\mu\sigma}$ are a pair of mutually dual scalar fields, and α is a short-distance cutoff of the bosonic theory.¹² Following Ref. 13, we pass to linear combinations of the bosonic fields describing the total and relative charge and spin excitations,

$$\Phi_c^\pm = \frac{1}{2} (\Phi_{+\uparrow} + \Phi_{+\downarrow} \pm \Phi_{-\uparrow} \pm \Phi_{-\downarrow}),$$

$$\Phi_s^\pm = \frac{1}{2} (\Phi_{+\uparrow} - \Phi_{+\downarrow} \pm \Phi_{-\uparrow} \mp \Phi_{-\downarrow}).$$

The kinetic energy of chiral Fermions then becomes the sum of four Gaussian models ($a = c^\pm, s^\pm$),

$$\mathcal{H}_{\text{kin}} = (v_F/2) \sum_a [(\partial_x \Theta_a)^2 + (\partial_x \Phi_a)^2], \quad (10)$$

while the dimerization operator takes the form:

$$\mathcal{O}_{\text{dim}} = (4/\pi\alpha) \times [\cos(\sqrt{\pi}\Phi_c^+) \cos(\sqrt{\pi}\Phi_c^-) \cos(\sqrt{\pi}\Phi_s^-) \cos(\sqrt{\pi}\Phi_s^+) + \sin(\sqrt{\pi}\Phi_c^+) \sin(\sqrt{\pi}\Phi_c^-) \sin(\sqrt{\pi}\Phi_s^-) \sin(\sqrt{\pi}\Phi_s^+)]. \quad (11)$$

As in the armchair case, the long-range part of the unscreened Coulomb interaction only involves the total charge field

$$H_{\text{Coul}} = \frac{2e^2}{\pi} \int dx \int dy \frac{\partial_x \Phi_c^+(x) \partial_y \Phi_c^+(y)}{|x-y|}, \quad (12)$$

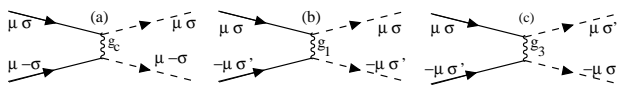


FIG. 3: The umklapp interaction g-ology: (a) in-chain, (b) inter-chain, no spin exchange, (c) inter-chain, spin exchange. The solid and dashed lines describe particles with opposite chiralities.

and greatly reduces the scaling dimension of the operator $\cos(\sqrt{4\pi}\Phi_c^+)$. At half filling, Umklapp processes contain this operator, and therefore become strongly relevant giving rise to a significant increase of all the gaps induced by interaction.^{6,7}

Turning to the uniform part of the short-range interaction (7), we single out contributions of umklapp processes, all of them proportional to the operator $\cos(\sqrt{4\pi}\Phi_c^+)$. This selection can be done by directly bosonizing (7), and can also be understood physically by using the g-ology approach (see Fig. 3). The result is:

$$\begin{aligned} \mathcal{H}_{\text{umkl}} = & -\frac{b}{(\pi\alpha)^2} \cos(\sqrt{4\pi}\Phi_c^+) \left\{ g_c \cos(\sqrt{4\pi}\Phi_c^-) \right. \\ & + (g_3 - g_1) \cos(\sqrt{4\pi}\Phi_s^+) + g_1 \cos(\sqrt{4\pi}\Phi_s^-) \\ & \left. - g_3 \cos(\sqrt{4\pi}\Theta_s^-) \right\}. \end{aligned} \quad (13)$$

Within our U - V model, the parameters are $g_1 = g_c = (U - 3V)/n$, $g_3 = U/n$. The slightly strange looking structure in the spin sector is an artifact of treating the non-Abelian $SU(2)$ symmetry group by means of Abelian bosonization; this symmetry becomes manifest upon refermionization (see next section).

Appendix A contains a discussion of the full structure of the interaction including the less relevant terms which we will ignore in the remainder of this paper. The only feature generated by this extra complexity is a minor logarithmic renormalization of the masses generated in the theory. This may be important for estimating quantities to be measured experimentally, but will not make a difference to any of the universal properties of the gapped ground state phases of the system and the quantum criticality separating them.

The staggered part of interaction (7) is contributed both by the spin-exchange and non-spin-exchange scattering processes. In the effective one-dimensional picture, the non-spin-exchange process is proportional to the sum $\sum_l (-1)^l n(l)n(l+1)$. Here $n(l)$ is the total local density that transforms in the continuum limit to $b[J(x) + (-1)^l M(x)]$, where $J = \sum_{\mu\sigma} (: R_{\mu\sigma}^\dagger R_{\mu\sigma} : + : L_{\mu\sigma}^\dagger L_{\mu\sigma} :)$ and $M = \sum_{\mu\sigma} (R_{\mu\sigma}^\dagger L_{\mu\sigma} + h.c.)$. The above sum then becomes $b \int dx [M, J]_{x, x+\alpha}$. The emerging point-split commutator is then estimated using Operator Product Expansion (see Appendix B) and is proportional to the single-particle dimerization operator (11)

$$[M, J]_{x, x+\alpha} \equiv \lim_{\alpha \rightarrow 0} \{M(x)J(x+\alpha) - J(x)M(x+\alpha)\}$$

$$= 2\mathcal{O}_{\text{dim}}(x). \quad (14)$$

A similar procedure results in the same operator for the spin-exchange processes. Within the U - V model the dimerization amplitude is $g_\Delta = V/2n$. We must stress again here that although \mathcal{O}_{dim} is a single particle dimerization operator, g_Δ is an *effective* coupling constant, arising from projecting the interactions on the hexagonal lattice onto the low-energy theory relevant for a zigzag nanotube. The *bare* coupling constant associated with this operator arising from curvature effects may then be safely neglected, as it is of order $1/n^2$, much less than the effective g_Δ .

Thus we arrive at the effective model describing the zigzag nanotube at half filling in the scaling limit,

$$\mathcal{H} = \mathcal{H}_{\text{kin}} + \mathcal{H}_{\text{Coul}} + \mathcal{H}_{\text{umkl}} + \mathcal{H}_\Delta, \quad (15)$$

where $\mathcal{H}_\Delta = g_\Delta \mathcal{O}_{\text{dim}}$.

III. ADIABATIC APPROXIMATION AND MAPPING TO SPIN SECTOR

The unscreened Coulomb interaction strongly enhances the velocity of the symmetric charge mode relative to the group velocities of collective excitations in other channels.¹⁴ Hence, from the point of view of the field Φ_c^+ , all other degrees of freedom can be regarded as static. This allows one to employ an adiabatic approximation and obtain the low-energy dynamics of the model by integrating out the total charge mode. Such a procedure has already been discussed for narrow-gap SWNTs away from half-filling¹⁵ ($\mathcal{H}_{\text{umkl}} = 0$) and for a half-filled armchair nanotube⁷ ($\mathcal{H}_\Delta = 0$). The general analysis of the model (15) represents a more complicated task due to the presence of two strongly relevant perturbations – the Umklapp and dimerization terms, each containing the field Φ_c^+ .

In this paper, we will specialize to the limit where $\mathcal{H}_{\text{umkl}}$ is the principal term, responsible for the formation of a fully gapped Mott phase, and then address the effect of \mathcal{H}_Δ as a perturbation on this phase.

Such an approach can be justified in our U - V model by choosing $U \gg V > 0$, because the structure of the Umklapp interaction (13) contains parts proportional to U , whereas the dimerization includes only the smaller V . The details of integrating out Φ_c^+ are well explained in Ref. 7. Here we give a basic physical argument that leads us to the correct result. By examining Eq.(13) and making the approximation that all other fields are static during the typical fluctuation time of Φ_c^+ , we obtain a modified sine-Gordon model describing the total charge field,

$$\mathcal{H} \sim \mathcal{H}_0[\Phi_c^+] - A \cos \sqrt{4\pi}\Phi_c^+. \quad (16)$$

Here $\mathcal{H}_0[\Phi_c^+]$ is the sum of a standard Gaussian model and the nonlocal Coulomb term (12), whereas A is a combination of the slower fields which, within the adiabatic

approximation, can be replaced by a constant. Due to the high velocity and low effective scaling dimension of the field Φ_c^+ , all the spectral gaps (i.e. those of solitons and breathers) in the total charge sector are very large. Therefore, to examine the low-energy dynamics of neutral modes, one can consider the field Φ_c^+ to be locked at $\Phi_c^+ = 0$ and replace cosines of this field by their expectation values.

It is important at this stage to consider the physics we are discarding by making this approximation. Charged solitons in the Φ_c^+ field do indeed exist in the theory. Furthermore, electron like quasi-particles described by a half soliton simultaneously in each of the sectors of the theory are also present. Finally, there will also be plasmonic excitations corresponding to breathers modes in Hamiltonian (16). However, due to the strong renormalization of the Φ_c^+ field, each of these excitations will have a large mass.

Thus, as we are interested in the low-energy properties of the model, the only excitations that remain are neutral collective modes: the relative charge ‘‘vortex’’ modes, and the spin degrees of freedom (which as we will see later can be separated into a singlet mode and a triplet mode), and it is in this region of energies below any of the charged excitations that the adiabatic approximation (and therefore the description in terms only of neutral modes) is valid. This also explains why the dimerization term \mathcal{H}_Δ with a magnitude much less than any of the charged excitations can not turn the system into a trivial band-insulator: everything occurs within the Mott phase. We now proceed to analyse the low-energy phase diagram of such a model, and show the existence of an interesting non-trivial quantum phase transition.

A. The Umklapp term

Following the procedure of Ref. 7, one can identify the remaining neutral collective modes at $g_\Delta = 0$ by introducing four real (Majorana) fermions $\chi_{R,L}^i$ ($i = 0, 1, 2, 3$) and refermionizing the theory. The resulting Hamiltonian displays an $SU(2) \times Z_2$ symmetry in the spin sector:

$$\begin{aligned} \mathcal{H}' = & \frac{v}{2} \left[(\partial_x \Theta_c^-)^2 + (\partial_x \Phi_c^-)^2 \right] - \frac{m_f}{\pi\alpha} \cos \sqrt{4\pi} \Phi_c^- \\ & + \frac{iv}{2} \sum_{i=0}^3 (-\chi_R^i \partial_x \chi_R^i + \chi_L^i \partial_x \chi_L^i) - im_t \sum_{a=1}^3 \chi_R^a \chi_L^a \\ & - im_s \chi_R^0 \chi_L^0. \end{aligned} \quad (17)$$

Here $m_f = \langle \cos(\sqrt{4\pi} \Phi_c^+) \rangle g_1 / \pi\alpha$ is the mass of the relative charge (‘‘vortex’’) excitation, whereas $m_t = \langle \cos(\sqrt{4\pi} \Phi_c^+) \rangle (g_1 - g_3) / \pi\alpha$ and $m_s = \langle \cos(\sqrt{4\pi} \Phi_c^+) \rangle (g_3 + g_1) / \pi\alpha$ are the masses of the spin-triplet and spin-singlet modes, respectively. In terms of our $U - V$ model, the masses are parametrized as follows:

$$m_s = C \frac{2U - 3V}{n}, \quad m_t = -C \frac{3V}{n}, \quad (18)$$

where $C = \langle \cos(\sqrt{4\pi} \Phi_c^+) \rangle \approx 1$.

Associated with the Majorana fermions are four Ising models characterized by order and disorder parameters, σ_i and μ_i . We use the correspondence:

$$\begin{aligned} \cos \sqrt{\pi} \Phi_s^+ &= \sigma_1 \sigma_2 & \sin \sqrt{\pi} \Phi_s^+ &= \mu_1 \mu_2 \\ \cos \sqrt{\pi} \Theta_s^+ &= \mu_1 \sigma_2 & \sin \sqrt{\pi} \Theta_s^+ &= \sigma_1 \mu_2 \\ \cos \sqrt{\pi} \Phi_s^- &= \sigma_0 \sigma_3 & \sin \sqrt{\pi} \Phi_s^- &= \mu_0 \mu_3 \\ \cos \sqrt{\pi} \Theta_s^- &= \mu_0 \sigma_3 & \sin \sqrt{\pi} \Theta_s^- &= \sigma_0 \mu_3. \end{aligned} \quad (19)$$

The sign of the Majorana mass indicates whether the corresponding Ising model is ordered ($m < 0$, $\langle \sigma \rangle \neq 0$, $\langle \mu \rangle = 0$) or disordered ($m > 0$, $\langle \mu \rangle \neq 0$, $\langle \sigma \rangle = 0$)¹⁶.

The fermionic part of the Hamiltonian (17) has the same structure as that of a two-leg antiferromagnetic spin-1/2 ladder.¹⁷ Indeed, assuming that $U/V \gg 1$, we find that $m_t < 0$ and $m_s > 0$ so that $\langle \sigma_a \rangle \neq 0$ for $a = 1, 2, 3$ and $\langle \mu_0 \rangle \neq 0$. Furthermore, $m_f > 0$ meaning that $\langle \cos(\sqrt{\pi} \Phi_c^-) \rangle \neq 0$. These signs of the masses indicate a spin-liquid behavior of the system.^{16,17} We can further quantify this by defining the staggered magnetization as a suitably averaged difference between the local spin densities on the two sublattices, $\mathbf{n}^-(\mathbf{r}) = \mathbf{S}_a(\mathbf{r}) - \mathbf{S}_b(\mathbf{r})$. Projecting this onto the low-energy sector of the model gives

$$\mathbf{n}^- \sim \cos(\sqrt{\pi} \Phi_{c^-}) \mu_0 (\mu_1 \sigma_2 \sigma_3, \sigma_1 \mu_2 \sigma_3, \sigma_1 \sigma_2 \mu_3). \quad (20)$$

The two-point correlation function of \mathbf{n}^- displays a coherent magnon peak with a mass gap $|m_t|$.

B. Effect of dimerization term

After refermionization the dimerization operator acquires the following low-energy form:

$$\mathcal{O}_{\text{dim}} \sim \cos(\sqrt{\pi} \Phi_c^-) \mu_0 \mu_1 \mu_2 \mu_3. \quad (21)$$

In the spin-liquid phase formed by the umklapp processes this operator can be further simplified by replacing in the leading order the operators $\cos(\sqrt{\pi} \Phi_c^-)$ and μ_0 by their expectation values. Thus, projecting \mathcal{O}_{dim} onto the spin-triplet sector yields

$$\begin{aligned} \mathcal{H}_\Delta &= h_{\text{eff}} \mu_1 \mu_2 \mu_3, \\ h_{\text{eff}} &= \frac{4g_\Delta}{(\pi\alpha)^2} \langle \cos(\sqrt{\pi} \Phi_c^+) \rangle \langle \cos(\sqrt{\pi} \Phi_c^-) \rangle \langle \mu_0 \rangle. \end{aligned} \quad (22)$$

We see that the dimerization term competes with umklapp processes which support the ground state with $\langle \sigma_i \rangle \neq 0$, $\langle \mu_i \rangle = 0$.

The resulting theory thus involves only the spin-triplet degrees of freedom and actually coincides with the problem of a two-leg spin ladder with explicit dimerization,⁹ or, equivalently, a weakly dimerized spin-1 chain with a small Haldane gap.¹⁰ It was shown that increasing the dimerization can drive the system towards a quantum criticality belonging to the universality class of the

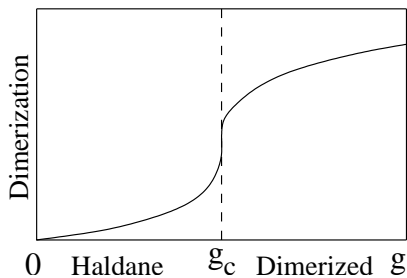


FIG. 4: Average dimerization as a function of $g = m_{\Delta}/m_t \sim n^{2/13}$, being nonzero in both gapped phases, displays a singularity in the derivative at the critical point $g = g_c$.

$SU(2)_1$ Wess-Zumino-Novikov-Witten model with central charge 1. Close to criticality the universal lowest-energy properties of the system are those of a single, explicitly dimerized, antiferromagnetic spin-1/2 chain, with the dimerization changing its sign across the transition.

The location of the critical point can be estimated by requiring that the mass gap generated by the dimerization term alone and the triplet mass become of the same order. Using standard scaling arguments we find that in Eq. (22) $h_{\text{eff}} \sim |m_f|^{1/4}|m_s|^{1/8}g_{\Delta}$, where all parameters in the right-hand side are proportional to $1/n$. Therefore the dimerization gap scales as

$$m_{dim} \sim h_{\text{eff}}^{8/13} \propto (1/n)^{11/13}, \quad (23)$$

and so, within our $U \gg V$ approximation

$$\frac{m_{\Delta}}{|m_t|} \propto \left(\frac{\bar{U}}{\bar{V}}\right)^{3/13} \left(\frac{n}{\bar{V}}\right)^{2/13}, \quad (24)$$

where $\bar{U} = U\alpha/v$ and $\bar{V} = U\alpha/v$ are dimensionless coupling constants.

This estimate shows that for sufficiently large radius n the dimerization is always dominant and the system occurs in a gapped phase whose properties are governed by the operator O_{dim} . Whether a crossover to the spin-liquid phase through the $SU(2)_1$ criticality can occur as a function of the nanotube's radius depends on various nonuniversal prefactors. As shown in Appendix A, an improved estimate of the critical line can be obtained by taking less relevant (non-umklapp) terms into account. The ratio of the dimerization and triplet mass gaps then becomes

$$\frac{m_{dim}}{|m_t|} \sim \frac{(\bar{V}/\bar{U})^{8/13}}{(\bar{U}/n)^{15/13} \ln(n/\bar{U})}. \quad (25)$$

The new estimate shows that the quantum transition scenario taking place upon decreasing n at large U is a real possibility.

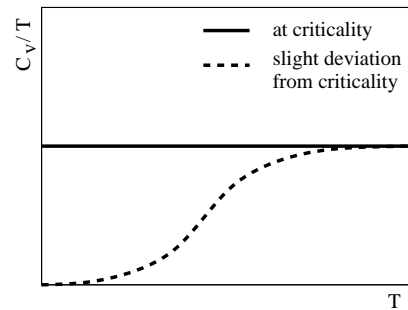


FIG. 5: C_v/T as a function of T . The solid line denotes the behavior exactly at criticality $g = g_c$, the dashed line is slightly away from criticality. The crossover temperature is given by the smallest gap in the system $m \sim |g - g_c|^{2/3}$.

C. Physical Observables

The ratio $g = m_{\Delta}/m_t$ acts as a control parameter for the quantum phase transition, with a critical point $g_c \sim 1$. As we vary g , the dimerization itself shows a singularity in its derivative as one passes through the transition point itself¹⁰ according to

$$\langle \mathcal{O}_{dim} \rangle = \langle O_{dim}(g = g_c) \rangle + \alpha |g - g_c|^{1/3} \text{sign}(g - g_c), \quad (26)$$

where α is some constant. This is qualitatively shown in Fig. 4.

The parameter g can be varied by varying the radius of the nanotube, n , or by changing the interaction coupling constants; the latter can be achieved by, for example, applying pressure or stretching the nanotube. The dimerization of the nanotube will show up as a Peierls distortion of the lattice, which should be measurable with low-temperature STM.

The proximity to the quantum critical point will also show up in thermodynamic quantities, such as specific heat. Exactly at the critical point, the specific heat is linear in temperature¹⁸

$$C_V(g = g_c) = c \frac{\pi T}{3v}, \quad (27)$$

where $c = 1$ is the central charge of the criticality, and v is the Fermi velocity. Away from criticality, the specific heat is exponentially small at sufficiently low temperature $T < m$,

$$C_V \sim T^{-3/2} e^{-m/T}, \quad (28)$$

where m is the smallest gap in the system, which near criticality is given¹⁰ by $m \sim |g - g_c|^{2/3}$. The specific heat crosses over to a linear dependence on temperature when $T > m$. This is plotted in Figure 5.

IV. CONCLUSIONS

We have shown that in zigzag carbon nanotubes electron-electron interactions play an important role in

the ground state of the system. Firstly, there is the long-range unscreened Coulomb interaction, which sets a hierarchy of energy scales in the problem. Secondly, there are umklapp processes (in the undoped case) which gap all collective excitations in the nanotube. Finally, there is an explicit dimerization in the interaction, scaling as $1/n$ due to the way that we break the C_3 symmetry when we wrap the zigzag nanotube. This dimerization originates from interactions and affects the effective low-energy action; there it directly competes with Umklapp processes supporting a Mott-like insulating phase with a spin-liquid structure of collective excitations.

As the relative strength of the dimerization is increased, the system can exhibit a nontrivial quantum criticality with an $SU(2)_1$ symmetry. On one side of this critical point, the system is in a Haldane spin liquid phase, on the other side of the critical point, the ground state is dimerized. The position in the phase diagram depends on the radius of the nanotube, with reasonable assumptions about parameters showing we are always near the QCP. Therefore, small external perturbations may be able to drive the real system of a zigzag carbon nanotube to an exciting theoretical quantum criticality.

V. ACKNOWLEDGEMENTS

We thank A.M.Tsvelik and F. Essler for stimulating discussions. STC's work is supported by the EPSRC grant GLGL RRAH 11382, and was partly done while STC was at ICTP. Part of this work was done during AAN's visit to Imperial College supported by EPSRC grant GR/N19359. AOG's work is partly supported by the EPSRC grant GR/R70309 by the EU training network DIENOW.

APPENDIX A: FULL STRUCTURE OF INTERACTION

The long range Coulomb interaction means that the gap in the total charge excitations is the largest energy scale in the problem, and consequently the umklapp terms which involve $\cos \sqrt{4\pi}\Phi_c^+$ are the most relevant terms which gap the remaining sectors of the theory. However, as the term which gaps the triplet sector is proportional to $V \ll U$, less relevant terms may strongly renormalize the triplet mass. In this section, we continue to assume that $U \gg V$, so that we only look at corrections proportional to U .

Bosonizing the interaction H_U (7) gives rise to the following addition to the Umklapp Hamiltonian (13)

$$\Delta H = \bar{U} \int dx \cos \sqrt{4\pi}\Phi_c^- \left(\cos \sqrt{4\pi}\Phi_s^+ + \cos \sqrt{4\pi}\Theta_s^- \right), \quad (\text{A1})$$

where \bar{U} is a dimensionless interaction constant $\bar{U} = Ub/(\pi\alpha)^2$.

The mass gap (in dimensionless units) associated with the relative charge sector is generated by the more relevant umklapp processes

$$m_f \approx C \frac{\bar{U}}{n} \quad (\text{A2})$$

where $C = \langle \cos \sqrt{4\pi}\Phi_c^+ \rangle \approx 1$, so we can assume that this field Φ_c^- becomes locked, and the expectation value

$$\langle \cos \sqrt{4\pi}\Phi_c^- \rangle \approx m_f \ln \frac{1}{m_f}. \quad (\text{A3})$$

After refermionization, ΔH will contribute to both the singlet mass and the triplet mass. As the singlet gap is already of order U/n , a change of order $(U/n)^2$ is insignificant. However, the triplet mass will become

$$m_t = -C \frac{3\bar{V}}{n} - C^2 \left(\frac{\bar{U}}{n} \right)^2 \ln \left(\frac{n}{\bar{U}} \right). \quad (\text{A4})$$

We considered in the main text the case where $V/n \gg (U/n)^2 \ln(n/U)$. If U is large enough, then the opposite limit may hold true, in which case the ratio of the dimerization and the triplet masses modifies and becomes given by formula (25).

APPENDIX B: THE OPERATOR PRODUCT EXPANSION

Here, we use the Operator Product Expansion (OPE) in the fermionic basis to show that the staggered interaction gives rise to a single particle dimerization term in the continuous limit.

The bare Hamiltonian in the Fermionic basis is

$$H_0 = -iv_F \sum_{\mu\sigma} \int dx [R_{\mu\sigma}^\dagger \partial_x R_{\mu\sigma} - L_{\mu\sigma}^\dagger \partial_x L_{\mu\sigma}], \quad (\text{B1})$$

so the Matsubara Green's functions are

$$\begin{aligned} \langle L_{\mu\sigma}^\dagger(z) L_{\mu'\sigma'}(w) \rangle &= \langle L_{\mu\sigma}(z) L_{\mu'\sigma'}^\dagger(w) \rangle = \frac{\delta_{\mu\mu'} \delta_{\sigma\sigma'}}{2\pi(z-w)} \\ \langle R_{\mu\sigma}^\dagger(\bar{z}) R_{\mu'\sigma'}(\bar{w}) \rangle &= \langle R_{\mu\sigma}(\bar{z}) R_{\mu'\sigma'}^\dagger(\bar{w}) \rangle = \frac{\delta_{\mu\mu'} \delta_{\sigma\sigma'}}{2\pi(\bar{z}-\bar{w})} \end{aligned} \quad (\text{B2})$$

where

$$z = v_F\tau + ix, \quad \bar{z} = v_F\tau - ix, \quad (\text{B3})$$

and similarly for w , are the complex coordinates written in a manifestly Lorentz invariant way, with τ being the imaginary time.

The first staggered piece in Eq. (7) takes the form

$$(-1)^l n(l)n(l+1), \quad (\text{B4})$$

where $n(l) = \sum_{\mu\sigma} n_{\mu\sigma}(l)$ is the total electron density at site l . In the continuum limit, this becomes

$$b[M(x)J(x+\alpha) - J(x)M(x+\alpha)], \quad (\text{B5})$$

where

$$\begin{aligned} J(x) &= \sum_{\mu\sigma} (J_{\mu\sigma}^R + J_{\mu\sigma}^L), \\ M(x) &= \sum_{\mu\sigma} (R_{\mu\sigma}^\dagger L_{\mu\sigma} + L_{\mu\sigma}^\dagger R_{\mu\sigma}). \end{aligned} \quad (\text{B6})$$

Therefore, in the expansion of (B5), we will need the following OPE:

$$\begin{aligned} &: L^\dagger(z)L(z) :: L^\dagger(w)R(w) : \\ &\sim \langle L(z)L^\dagger(w) \rangle : L^\dagger(z)R(z) := \frac{1}{2\pi(z-w)} : L^\dagger(z)R(z) :, \\ &: L^\dagger(z)L(z) :: R^\dagger(w)L(w) : \\ &\sim -\langle L^\dagger(z)L(w) \rangle : R^\dagger(z)L(z) := \frac{-1}{2\pi(z-w)} : R^\dagger(z)L(z) :, \end{aligned}$$

where the flavor and spin subscripts must all be identical. Similar OPE's hold for the antianalytic part of the expansion, so that

$$\begin{aligned} J(z)M(w) &\sim \frac{1}{2\pi} \left(\frac{1}{z-w} - \frac{1}{\bar{z}-\bar{w}} \right) \\ &\times \sum_{\mu\sigma} : (R_{\mu\sigma}^\dagger L_{\mu\sigma} - L_{\mu\sigma}^\dagger R_{\mu\sigma}) :. \end{aligned} \quad (\text{B8})$$

We recognise the operator as the dimerization operator, hence putting $\tau = 0$ and evaluating the point-split commutator in (B5), we see that

$$\begin{aligned} [M, J]_{x, x+\alpha} &\equiv \lim_{\alpha \rightarrow 0} \{M(x)J(x+\alpha) - J(x)M(x+\alpha)\} \\ &= 2O_{\text{dim}}(x). \end{aligned} \quad (\text{B9})$$

The other component of the staggered interaction

$$\begin{aligned} &(-1)^l c_{\mu\sigma}^\dagger(l) c_{-\mu\sigma}(l) c_{-\mu\sigma'}^\dagger(l+1) c_{\mu\sigma'}(l+1) \\ &= b^2 \left[(R_{\mu\sigma}^\dagger L_{-\mu\sigma} + L_{\mu\sigma}^\dagger R_{-\mu\sigma})_x (R_{-\mu\sigma'}^\dagger R_{\mu\sigma'} + L_{-\mu\sigma'}^\dagger L_{\mu\sigma'})_{x+\alpha} \right. \\ &\quad \left. - (R_{\mu\sigma}^\dagger R_{-\mu\sigma} + L_{\mu\sigma}^\dagger L_{-\mu\sigma})_x (R_{-\mu\sigma'}^\dagger L_{\mu\sigma'} + L_{-\mu\sigma'}^\dagger R_{\mu\sigma'})_{x+\alpha} \right] \end{aligned} \quad (\text{B10})$$

can be treated in an identical way. This too turns into the dimerization operator, giving the final result quoted in the main text.

¹ S.Ijima, Nature **54**, 56 (1991).

² C.Dekker, Phys. Today **52**, 22 (1999).

³ R.Saito, G.Dresselhaus and M.S.Dresselhaus, *Physical properties of carbon nanotubes* (Imperial College Press, 1998).

⁴ R.Egger and A.O.Gogolin, Phys. Rev. Lett. **79**, 5082 (1997); R.Egger and A.O.Gogolin, Euro. Phys. J. B **3** 281 (1998); C.Kane, L.Balents and M.P.A.Fisher, Phys. Rev. Lett. **79**, 5086 (1997).

⁵ M.Bockrath, D.H.Cobden, J.Lu, A.G.Rinzlar, R.E.Smalley, L.Balents and P.L.McEuan, Nature **397**, 598 (1999).

⁶ H.Yoshioka and A.Odintsov, Phys. Rev. Lett. **82**, 374 (1999); A.Odintsov and H.Yoshioka, Phys. Rev. B **59**, R10 457 (1999).

⁷ A.A.Nersesyan and A.M.Tsvetik, Phys. Rev. B **68**, 235419 (2003).

⁸ C.L.Kane and E.J.Mele, Phys. Rev. Lett. **78**, 1932 (1997).

⁹ M.A.Martin-Delgado, R.Shankar and G.Sierra, Phys. Rev. Lett. **77**, 3443 (1996).

¹⁰ Y.-J.Wang and A.A.Nersesyan, Nucl. Phys. B **583**, 671 (2000).

¹¹ H.H.Lin, Phys. Rev. B **58**, 4963 (1998).

¹² In the non-interacting case, $b = \pi\alpha$. In the presence of interactions, this relationship changes in a non-universal way, however the two parameters stay within the same order of magnitude and the difference between them is not important for the purposes of this paper.

¹³ V.J.Emery and S.A.Kivelson, Phys. Rev. B **46**, 10812 (1992).

¹⁴ L. Glazman *et al*, Phys. Rev. B **45**, 8454 (1992); H.J. Schulz, Phys. Rev. Lett. **71**, 1864 (1993).

¹⁵ L.S.Levitov, A.M.Tsvetik, Phys. Rev. Lett. **90**, 016401 (2003).

¹⁶ A.O.Gogolin, A.A.Nersesyan and A.M.Tsvetik *Bosonization and strongly correlated systems* (Cambridge University Press, 1998).

¹⁷ D.Shelton, A.A.Nersesyan and A.M.Tsvetik, Phys. Rev. B **53**, 8521 (1996).

¹⁸ I.Affleck, Phys. Rev. Lett. **56**, 746 (1986); H.W.J. Blöte,

J.L. Cardy and M.P. Nightingale, *ibid.* **56**, 742 (1986).